Generation and rescue of a murine model of platelet dysfunction: The Bernard-Soulier syndrome

Jerry Ware*, Susan Russell, and Zaverio M. Ruggeri

Roon Research Center for Arteriosclerosis and Thrombosis, Division of Experimental Hemostasis and Thrombosis, Departments of Molecular and Experimental Medicine and of Vascular Biology, The Scripps Research Institute, La Jolla, CA 92037

Communicated by Ernest Beutler, The Scripps Research Institute, La Jolla, CA, December 30, 1999 (received for review October 7, 1999)

The human Bernard-Soulier syndrome is an autosomal recessive disorder of platelet dysfunction presenting with mild thrombocytopenia, circulating ''giant'' platelets and a bleeding phenotype. The bleeding in patients with the Bernard-Soulier syndrome is disproportionately more severe than suggested by the reduced platelet count and is explained by a defect in primary hemostasis owing to the absence of the platelet glycoprotein (GP) Ib-IX-V membrane receptor. However, the molecular basis for the giant platelet phenotype and thrombocytopenia have remained unresolved but assumed to be linked to an absent receptor complex. We have disrupted the gene encoding the α-subunit of mouse GP Ib-IX-V (GP Ibα) and describe a murine model recapitulating the hallmark characteristics of the human Bernard-Soulier syndrome. The results demonstrate a direct link between expression of a GP Ib-IX-V complex and normal megakaryocytopoiesis and platelet morphogenesis. Moreover, using transgenic technology the murine Bernard-Soulier phenotype was rescued by expression of a human GP Ibα subunit on the surface of circulating mouse platelets. Thus, an *in vivo* model is defined for analysis of the human GP Ib-IX-V receptor and its role in the processes performed exclusively by megakaryocytes and platelets.

The human Bernard-Soulier syndrome was described more than 50 years ago as a severe, and potentially fatal, inherited bleeding disorder with mild thrombocytopenia and the presence of "giant" platelets in peripheral blood smears (1). The bleeding is caused by an inherent platelet defect characterized by an inability of platelets to agglutinate in the presence of ristocetin, a common laboratory procedure used to characterize platelet function (2, 3). The defect responsible for the lack of ristocetin-mediated platelet function is an absent platelet membrane receptor, the glycoprotein (GP) Ib-IX-V complex, and an inability of platelets to agglutinate through an interaction with plasma von Willebrand factor (4, 5). Indeed, the presence of von Willebrand factor at sites of vascular injury supports normal hemostasis by binding to the platelet GP Ib-IX-V complex, which, in turn, tethers circulating platelets from flowing blood onto a damaged vascular surface (6–8).

The Bernard-Soulier syndrome is inherited as an autosomal recessive trait and is associated with a growing database of heterogeneous mutations within the individual subunits of the GP Ib-IX-V receptor (3). The receptor is encoded by four separate gene products, the α- and β-subunits of GP Ib, GP IX, and GP V (9). Single mutations within genes encoding either subunit of GP Ib or GP IX have been associated with the Bernard-Soulier syndrome, and the net effect of these mutations is a functional loss of von Willebrand factor binding to the complex (3). Whether other aspects of the Bernard-Soulier syndrome, such as the macrothrombocytopenia, are a direct result of an absent GP Ib-IX-V receptor has not been established. Indeed, there are a number of seemingly unrelated macrothrombocytopenic disorders not associated with a dysfunctional GP Ib-IX-V receptor and their molecular basis has remained unresolved (10–13).

The current study was undertaken to develop an animal model of the Bernard-Soulier syndrome and determine whether the pleiotropic phenotype that is typical of the Bernard-Soulier syndrome can be explained by a single defect in the GP Ib-IX-V complex. The results provide experimental proof that the bleeding, thrombocytopenia, and giant platelets are all a direct result of an absent GP Ib-IX-V receptor. The mouse model of the Bernard-Soulier syndrome could be rescued with transgenic expression of a human α-subunit (GP Ibα) and, as such, defines an experimental framework to manipulate human platelet receptors in the *in vivo* setting of the mouse megakaryocyte and platelet.

Materials and Methods

Targeting Vector. The characterization and isolation of the mouse GP Ibα gene has been described (14, 15). The mouse GP Ibα gene was altered by site-directed mutagenesis to insert unique restriction sites flanking the coding sequence. This strategy allowed a complete replacement of GP Ibα coding sequence with a phosphoglycerate kinase-neo^r cassette (provided by Richard Hynes, Massachusetts Institute of Technology, Cambridge). Electroporation of embryonic stem (ES) cells was performed by Genome Systems (St. Louis), and G418-resistant colonies were screened by Southern analysis using probes from the 5′ region of the mouse GP Ibα gene. Based on Southern analysis results, cell lines were chosen for microinjection into mouse blastocysts. The injections were performed by the Transgenic Core Facility at The Scripps Research Institute.

Southern and Northern Analyses. Mouse tail DNA was isolated by using a QIAamp DNA isolation kit (Qiagen, Valencia, CA) and digested by using restriction enzymes purchased from New England Biolabs. Digested DNA was electrophoresed through a 0.8% agarose gel and transferred to nitrocellulose by a Southern transfer (16). A radiolabeled probe corresponding to nucleotides 1948–2659 of the mouse GP Ibα gene (numbers refer to GenBank accession no. U91967) was labeled by using [α-^{32}P]dATP and Prime-It Labeling kit from Stratagene. For the isolation of bone marrow RNA-dissected femur bones were immediately frozen in liquid nitrogen and pulverized in a porcelain mortar by using a pestle. After evaporation of the liquid nitrogen, the femur powder was dissolved in 4 M guanidinium isothiocyanate/0.1 M Tris, pH 7.5/0.5% *n*-lauroyl sarcosine. A centrifugation was performed to remove the large particulate matter of bone, and the supernatant was applied to a CsCl cushion to purify the total RNA (17). The RNA was electrophoresed through a 1% agarose/formaldehyde denaturing gel and transferred to nitrocellulose for hybridization (18). Radiolabeled DNA fragments

Abbreviations: GP, glycoprotein; ES, embryonic stem.

*To whom reprint requests should be addressed at: Mail Drop MEM 175, The Scripps Research Institute, 10550 North Torrey Pines Road, La Jolla, CA 92037. E-mail: jware@scripps.edu.

The publication costs of this article were defrayed in part by page charge payment. This article must therefore be hereby marked "*advertisement*" in accordance with 18 U.S.C. §1734 solely to indicate this fact.

Article published online before print: *Proc. Natl. Acad. Sci. USA*, 10.1073/pnas.050582097. Article and publication date are at www.pnas.org/cgi/doi/10.1073/pnas.050582097

corresponding to the coding sequence of mouse GP Ibα (Ser^{108} to Thr^{300} encoded by nucleotides 3035–3613) were prepared. After hybridization and washing the Southern and Northern filters were subjected to autoradiography and a photograph of the autoradiograph is presented.

Bleeding Time Assays. Mouse tail bleeding times were determined by removing 1–3 mm of distal mouse tail and immediately immersing the tail in 37°C isotonic saline. A complete cessation of bleeding was defined as the bleeding time. Bleeding time measurements exceeding 10 min were stopped by cauterization of the tail.

Light and Electron Microscopy. Whole blood was obtained from a periorbital puncture of anesthetized mice. Blood was collected into heparin-coated capillary tubes and transferred to a citrate/dextrose anticoagulant. Blood smears were prepared and briefly air-dried before being stained with Wright-Giemsa. Bone marrow cells were obtained from dissected femurs and immediately fixed in 1.5% glutaraldehyde buffered with 0.1 M sodium cacodylate for 30 min on ice. The cell pellet was postfixed in 1% OsO_4, dehydrated in graded alcohols, and embedded in polybed resin overnight.

Generation of Mice Deficient in Murine GP Ibα and Expressing a Human Transgene. The generation and characterization of transgenic mice expressing the human GP Ibα polypeptide ($hGPIb\alpha^{Tg}$) in the presence of two normal mouse GP Ibα alleles ($mGPIb\alpha^{wt}$) has been reported (19). To characterize the consequence of expressing a human transgene in the absence of an endogenous murine GP Ibα polypeptide, crosses were made to remove the coding sequence for the mouse GP Ibα polypeptide. As a first step, GP $Ib\alpha^{null}$ mice ($mGPIb\alpha^{null}$) were bred to mice containing the human transgene ($mGPIb\alpha^{wt}$;$hGPIb\alpha^{Tg}$). Southern blot analysis of the offspring confirmed the presence of heterozygous murine GP Ibα alleles whereas immunologic screening using anti-human GP Ibα mAbs identified mice also expressing the human transgene product ($mGPIb\alpha^{het}$;$hGPIb\alpha^{Tg}$). Mice containing heterozygous murine GP Ibα alleles and a functional human transgene were again crossed with GP $Ib\alpha^{null}$ mice (mGP $Ib\alpha^{het}$;$hGPIb\alpha^{Tg}$) × (mGP $Ib\alpha^{null}$), and the resultant offspring were genotyped and immunologically screened. This analysis identified mice with a murine GP $Ib\alpha^{null}$ locus and a functional human transgene ($mGPIb\alpha^{null}$;$hGPIb\alpha^{Tg}$).

FACscan Analysis and mAbs. A mAb labeled with FITC and recognizing the mouse integrin α_{IIb} subunit was obtained from PharMingen. Antibodies recognizing the human GP Ibα subunit were developed by this laboratory and have been described (20).

Results

Targeted Replacement of the Murine GP Ibα Gene. The murine GP Ibα gene is composed of two exons with the second exon encoding the 718-residue precursor polypeptide (14). A targeting vector to promote homologous recombination in murine ES cells was constructed in which the entire GP Ibα coding sequence was replaced with a phosphoglycerate kinase-neomycin-resistance (*neo*^{r}) cassette (Fig. 1*A*). The targeting vector supports positive ES cell selection from the presence of a *neo*^{r} cassette and negative selection from a thymidine kinase cassette placed 3′ to the GP Ibα gene. Accordingly, successful homologous recombination after transfection with the targeting vector would generate ES cellular DNA in which a 9-kb *Hin*dIII DNA fragment is replaced with a 6.7-kb *Hin*dIII fragment (Fig. 1*A*). Southern analysis of ES cell DNA isolated from G418-resistant colonies revealed a *Hin*dIII restriction pattern consistent with the successful replacement of the GP Ibα gene. In total, 180 different ES colonies were screened, and six revealed the

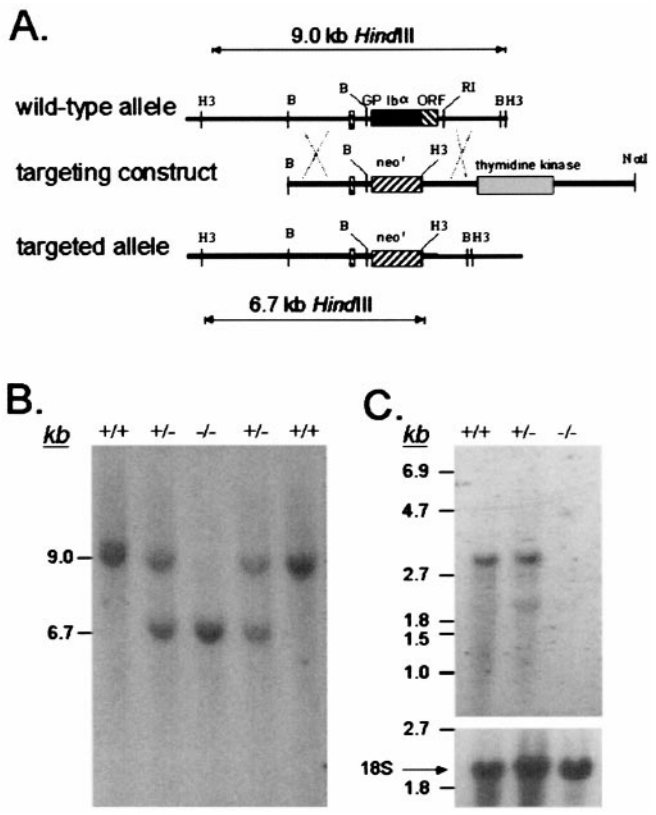

Fig. 1. Targeted deletion of the mouse GP Ibα gene. (*A*) A 9-kb region of the mouse GP Ibα locus was characterized by restriction enzyme (B = *Bam*HI, H3 = *Hin*dIII, RI = *Eco*RI) and DNA sequence analysis (14, 15). The nucleotide sequence was determined for a 5.4-kb region spanning 2.4 kb 5′ to exon I and 1.7 kb 3′ to exon II (exons indicated as boxes, with the ORF highlighted as a black box in the wild-type allele). A targeting construct was generated by an exact replacement of the GP Ibα ORF with a phosphoglycerate kinase-neo^r cassette (neo^r). A phosphoglycerate kinase-thymidine kinase gene cassette was inserted 3′ to the GP Ibα gene for selection against random integration using gancyclovir. A successfully targeted GP Ibα locus contains a 6.7-kb *Hin*dIII restriction fragment as compared with a 9-kb fragment in the wild-type locus. (*B*) ES cells with a targeted GP Ibα locus were identified by Southern hybridization and injected into blastocysts to generate chimeric mice. Germ-line transmission of the altered GP Ibα allele produced mice with heterozygous GP Ibα alleles. Heterozygous mice were bred to each other to generate a GP Ibα knockout mouse colony. Shown is a representative autoradiograph of mouse DNA digested with *Hin*dIII and hybridized with probes flanking the mouse GP Ibα gene. The results provide examples of the wild-type GP Ibα genotype (+/+), a heterozygous GP Ibα locus (+/−), and a homozygous-deficient GP Ibα locus (−/−). (*C*) Northern analysis of bone marrow isolated from the three representative GP Ibα genotypes is shown. The RNA was electrophoresed through a denaturing 1% agarose/formaldehyde gel and hybridized to probes from the coding region of the mouse GP Ibα gene. A transcript of approximately 2.8 kb is seen in both normal and heterozygous animals, but absent in RNA from GP Ibα knockout mice. The same filter was reprobed with a radiolabeled fragment of the 18S rRNA gene to demonstrate a similar load of RNA in each gel lane.

targeted substitution outlined in Fig. 1*A*. Characterization using additional restriction enzymes and Southern analysis provided supporting data for the likelihood that each of the six ES cells lines contained a replaced GP Ibα allele.

Three transformed ES cell lines were chosen for injection into C57BL/6 blastocysts. Chimeras from two of the three cell lines demonstrated germ-line transmission and altered GP Ibα alleles. Mice containing heterozygous GP Ibα loci (GP $Ib\alpha^{het}$) were bred (GP $Ib\alpha^{het}$ × GP $Ib\alpha^{het}$) and DNA analysis of the resultant offspring revealed all three expected GP Ibα genotypes: wild-

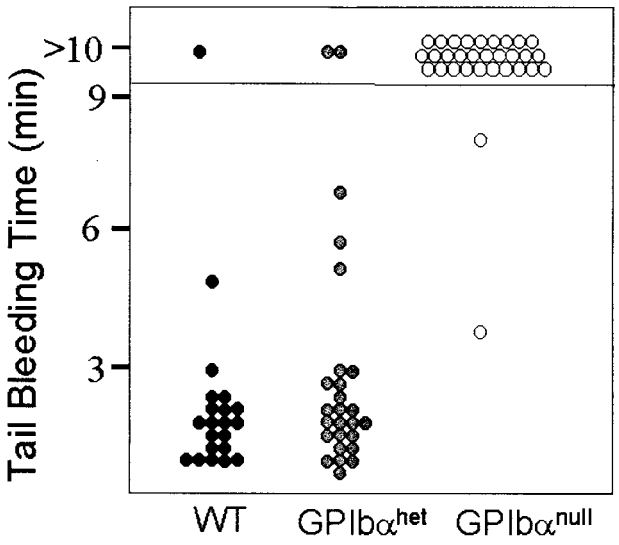

Fig. 2. Tail bleeding assays. Mice generated from the crossing of GP Ibα-heterozygous animals were analyzed in tail bleeding assays. After a blind determination of the bleeding time, tail DNA was isolated and genotyped by Southern analysis as shown in Fig. 1*B*. Shown are the times obtained for the three representative genotypes with each point representing an individual mouse. Normal mice (WT) and mice with heterozygous GP Ibα alleles (GP Ibα^{het}) show bleeding times that are similar to each other with the majority of times in the 1- to 3-min range. GP Ibα-deficient mice (GP Ibα^{null}) display a severe bleeding phenotype with 29 of 31 mice having bleeding times in excess of 10 min.

type (GP Ibα^{wt}), heterozygous (GP Ibα^{het}), and homozygous-deficient (GP Ibα^{null}) animals (Fig. 1*B*). Subsequent Northern analysis of bone marrow RNA confirmed successful GP Ibα gene deletion with the complete absence of GP Ibα mRNA in homozygous-deficient animals (Fig. 1*C*).

Phenoptypic Characterization of GP Ibα-Deficient Mice. Homozygous GP Ibα-deficient mice were viable and fertile and displayed no gross anatomical anomalies. Breeding between GP Ibα-deficient mice yielded normal-sized litters, suggesting the absence of GP Ibα is not associated with any significant embryonic lethality. To examine the hematostatic consequences of a murine GP Ibα deficiency, initial studies determined tail bleeding times. As shown in Fig. 2, bleeding times for wild-type mice and mice lacking a single GP Ibα allele were in the 1- to 3-min range. In contrast, 29 of 31 GP Ibα-deficient mice had bleeding times in excess of 10 min, typical of a severe bleeding phenotype. The complete hematologic profile of GP Ibα-deficient mice revealed normal red and white cell counts, normal hemoglobin, and a normal hematocrit (Table 1). In contrast, platelet counts were reduced and depended on the number of GP Ibα alleles present. GP Ibα-deficient platelet counts averaged 4.3×10^5 per μl of whole blood, whereas wild-type litter mates (GP Ibα^{wt}) produced from the breeding of GP Ibα-heterozygous animals averaged 1.5×10^6 per μl. Mice with heterozygous GP Ibα alleles had an intermediate platelet count averaging 1.0×10^6 per μl (Table 1).

The third characteristic of the human Bernard-Soulier syndrome, giant platelets, was observed in peripheral blood smears from GP Ibα^{null} animals (Fig. 3 *A* and *B*). Variable platelet sizes were seen with the largest platelets approaching the diameter of an erythrocyte. The complete profile of platelet sizes is presented by FACscan analysis and monitoring of the forward-light scattering profile as an indicator of particle (platelet) size (Fig. 3*C*).

Table 1. Blood counts

	WT	GP Ibα^{het}	GP Ibα^{null}
RBC, $\times 10^6/\mu$l	9.1 (0.6)	8.1 (0.4)	8.1 (0.6)
	$n = 4$	$n = 4$	$n = 4$
Hg, g/dl	15.0 (0.20)	14.2 (0.5)	14.6 (0.7)
	$n = 4$	$n = 4$	$n = 4$
PCV, % microhematocrit	42.3 (2.4)	38.1 (1.1)	38.1 (1.5)
	$n = 4$	$n = 4$	$n = 4$
WBC, $\times 10^3/\mu$l	9.1 (2)	10.4 (1)	8.4 (5)
	$n = 4$	$n = 4$	$n = 4$
Platelets, $\times 10^3/\mu$l	1,487 (134)	1,044 (104)	427 (86)
	$n = 12$	$n = 5$	$n = 9$

The mean is given with the SD in parentheses. WT, wild type; RBC, red blood cells; Hg, hemoglobin; PCV, packed cell volume; WBC, white blood cells.

GP Ibα Deficiency Results in a Primary Defect in the Maturing Megakaryocyte. The increase in platelet size resulting from GP Ibα deficiency suggests a defect in megakaryocytopoiesis or an inability of the circulating platelet to maintain normal morphology. To address either case in more detail, bone marrow megakaryocytes and platelets were prepared from normal and GP Ibα-deficient mice. Transmission electron microscopy revealed abnormal megakaryoctytes in GP Ibα-deficient mice lacking the typical developing platelet fields observed in a normal mature megakaryocyte (Fig. 4). The demarcating membrane system of GP Ibα-deficient megakaryocytes appeared

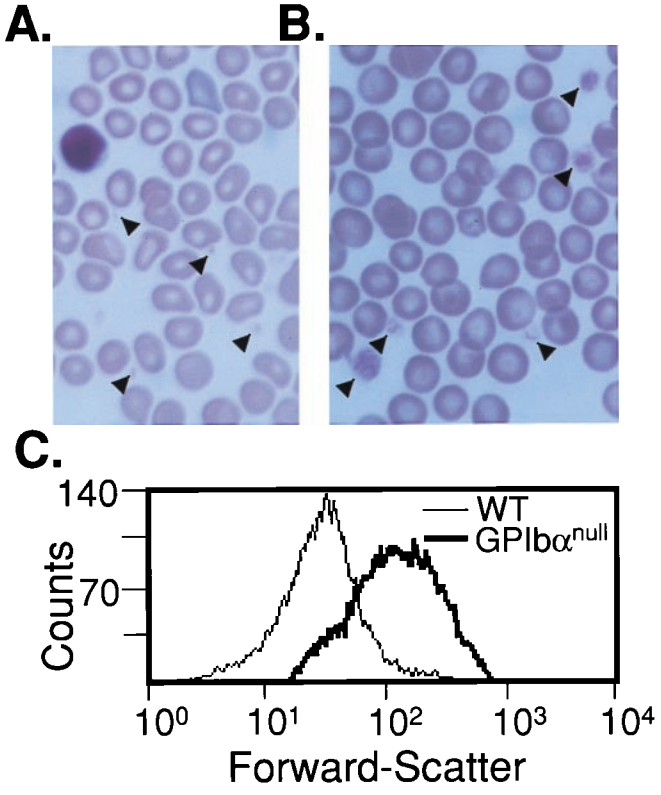

Fig. 3. Giant platelets in the GP Ibα-deficient mice. Stained peripheral blood smears from normal mice (*A*) and GP Ibα-deficient mice (*B*) are shown. Representative platelets are highlighted by arrows. (*C*) Forward-light scattering profiles from mouse platelets displays the entire population of platelet sizes in wild-type (WT) and GP Ibα-deficient (GP Ibα^{null}) mice. The platelet population was identified by using an anti-mouse CD41 (integrin α_{IIb} chain) mAb. Fifty thousand recorded events are presented for each genotype. A progressive shift to the right illustrates increasing platelet size.

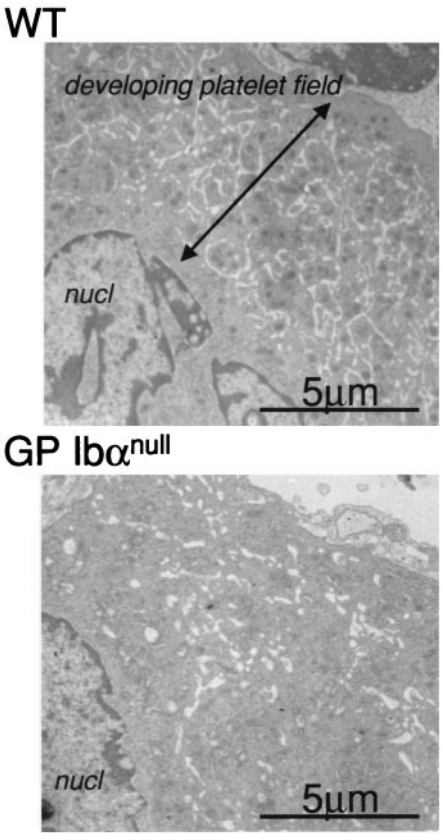

Fig. 4. Transmission electron microscopy of mature megakaryocytes. Bone marrow from mouse femurs was isolated and prepped for electron microscopy. Shown is a portion of a single mature megakaryocyte from a normal mouse (WT) and a GP Ibα-deficient mouse (GP Ibα^{null}). Nuclear material is shown (*nucl*) along with the developing platelet field and demarcation membrane system in a normal megakaryocyte cytoplasm. GP Ibα-deficient animals are devoid of a normal developing platelet field.

"vacuolated" or "disordered," confirming the association between GP Ibα expression (and/or the entire GP Ib-IX-V complex) and normal megakaryocytopoiesis. When compared with normal platelets, no changes in GP Ibα-deficient platelet ultrastructure were apparent beyond the size differences (data not shown).

Rescue of the Murine Bernard-Soulier Phenotype with a Human Transgene. We previously have reported transgenic expression of the human GP Ibα polypeptide on the surface of murine platelets (19). In the previous report, we established the ability of the human GP Ibα subunit to assemble with the murine GP Ibβ subunit to generate a chimeric GP Ib molecule on the surface of mouse platelets. Using a transgenic colony to express a human transgene (hGPIbα^{Tg}), we performed selective crosses to generate circulating mouse platelets expressing a human GP Ibα polypeptide but devoid of the endogenous murine GP Ibα subunit (see *Materials and Methods*). Such mice were identified (mGPIbα^{null};hGPIbα^{Tg}) and a representative GP Ibα FACscan profile illustrating the presence of the transgene product is shown (Fig. 5*A*).

Assays of mGPIbα^{null};hGPIbα^{Tg} mice were performed to characterize the function of the chimeric GP Ib molecule. Circulating platelet counts were increased to 8.4×10^5 per μl ($n = 12$; SD 1.29×10^5) representing an approximate 2-fold increase above counts obtained from mice with a GP Ibα^{null} genotype. The forward-scattering profile revealed a population of platelets similar in size to platelets from normal mice (Fig. 5*B*). Tail bleeding times were corrected to normal levels (compare Fig. 5*C* to Fig. 2). Thus, by these parameters the expression of the human transgene resulted in a correction of the aberrant platelet phenotype.

Discussion

The characterization of GP Ibα-deficient mice has revealed a recapitulation of the salient phenotypic features associated with the human Bernard-Soulier syndrome. Our studies demonstrate the GP Ib-IX-V complex directly participates in megakaryocyte maturation and platelet morphogenesis while providing additional evidence for the *in vivo* role of the platelet GP Ib-IX-V complex in normal hemostasis. Moreover, the correction of the mouse Bernard-Soulier phenotype with an expressed human transgene provides evidence that the disrupted molecular basis of the macrothrombocytopenia and bleeding are strictly conserved between both species. Thus, the mouse Bernard-Soulier syndrome mirrors the human disorder and is validated as a model to analyze the role of human GP Ibα in normal megakaryocyte and platelet biology.

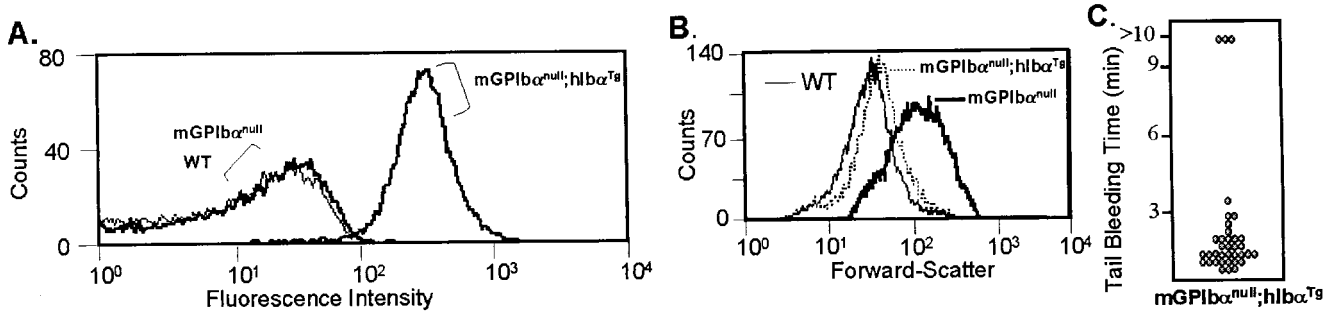

Fig. 5. Rescue of the GP Ibα-deficient phenotype with a human GP Ibα transgene. Transgenic mice expressing a human GP Ibα polypeptide under the control of a platelet-specific gene promoter have been reported (19). Mice expressing the human transgene but devoid of murine GP Ibα were generated by selective crosses of the transgenic mice and GP Ibα^{null} mice (see *Materials and Methods*). (*A*) A FACscan profile illustrates the reactivity of LJ-Ib1 (an anti-human GP Ibα mAb) with platelets from normal mice (WT), GP Ibα^{null} mice, and GP Ibα^{null} mice expressing the human transgene (mGPIbα^{null};hIbα^{Tg}). (*B*) FACscan analysis was performed on anticoagulated whole blood by using a platelet-specific anti-CD41 mAb (same as Fig. 3*C*). The forward-scattering profile of the fluorescent platelet population is shown as an indicator of particle or platelet size. The mGP Ibα^{null};hIbα^{Tg} profile is similar to that obtained from normal mice (WT), illustrating a correction in the platelet population size dependent on expression of the human transgene. (*C*) The results from bleeding times assays for mGPIbα^{null};hIbα^{Tg} mice are shown.

GP Ibα^{null} mice have circulating giant platelets, demonstrating the abnormal platelet morphology typical of the Bernard-Soulier syndrome is a consequence of an absent GP Ib-IX-V complex. The disordered and vacuolated demarcation membrane system of GP Ibα^{null} megakaryocytes is similar to reports of the aberrant ultrastructure observed for human megakaryocytes prepared from Bernard-Soulier syndrome patients (21). The abnormality in the murine megakaryocytes appears to be less dramatic than the megakaryocytic abnormalities observed in GATA-1-deficient mice, which probably reflects a more global megakaryoctye dysfunction generated by inactivation of the crucial transcription factor, GATA-1 (22). It is tempting to speculate that a disrupted linkage between the cytoplasmic tail of GP Ibα and components of the platelet membrane cytoskeleton, specifically actin-binding protein (23), might be the molecular cause of abnormal megakaryocytes in the murine Bernard-Soulier syndrome. However, an equally plausible explanation would be uncharacterized extracytoplasmic interactions between GP Ibα and the bone marrow matrix. A role for the GP Ibα extracytoplasmic domain in platelet formation has been suggested by the *in vitro* ability of antibodies recognizing the extracytoplasmic domain of GP Ibα to inhibit and alter megakaryocyte colony and proplatelet formation (24).

GP Ibα^{null} mice have a mild thrombocytopenia with circulating platelet counts approximating 30% the normal level (Table 1). As is the case for the human Bernard-Soulier syndrome, the bleeding phenotype is disproportionately more severe than the mild thrombocytopenia. A similar percent reduction in platelet count is common for the human disease even though normal human platelet counts are only one-fourth a normal mouse count (25). However, the contribution of platelet membrane surface to whole blood for each species is not as dramatically different as the difference in platelet count would suggest owing to the smaller size of mouse platelets. It is reported that mouse platelets have a mean platelet volume that is 60% of the mean volume of human platelets (26). Regardless, a similar percent reduction in platelet count suggests the thrombocytopenia associated with both the human and mouse Bernard-Soulier syndromes results from the same defect normally mediated by the GP Ib-IX-V complex. In fact, the thrombocytopenia and release of giant platelets in the Bernard-Soulier syndrome both may be the consequence of a single molecular defect normally mediated by an intact GP Ib-IX-V complex. As such, the single defect alters megakaryocyte maturation and impairs normal platelet morphogenesis, resulting in the macrothrombocytopenia (27).

Tail bleeding time was used as an assessment of the hemostatic function in GP Ibα^{null} mice, and by this criteria the mice have a severe bleeding phenotype. The prolonged bleeding time is similar to that observed with mice containing a disrupted β_3-subunit of the platelet $\alpha_{IIb}\beta_3$ integrin receptor (28). However, unlike the β_3 knockout we have observed no placental defects, which presumably reflects the role of a β_3-subunit in other non-$\alpha_{IIb}\beta_3$ integrin receptors and we have observed no evidence of spontaneous bleeding (28). The bleeding phenotype reported for GP Ibα^{null} mice has not been a problem for viability, breeding, or the normal handling of mice, but is apparent with a severe hemostatic challenge, such as that incurred during a determination of the bleeding time. Although differences undoubtedly will exist between mouse and human hemostasis (25), the characterizations presented in this work support key similarities between the human and mouse GP Ib-IX-V complexes and their role in platelet function.

Our decision to disrupt the mouse GP Ibα gene, as opposed to other subunits of the complex, was based on known aspects of human GP Ib-IX-V biology and the Bernard-Soulier syndrome (3). Foremost, mutations in the human GP Ibα gene are the most common molecular defect associated with the Bernard-Soulier syndrome. Typically, mutations in GP Ibα result in a complete absence of the surface expressed GP Ib-IX-V complex (3). The preponderance of mutations within the GP Ibα gene may reflect the larger size of the GP Ibα gene as compared with the GP Ibβ or GP IX genes, but also may be related to the functional dominance of the GP Ibα subunit within the complex. Well-characterized binding sites for von Willebrand factor, thrombin, a member of the 14–3-3 protein family, and actin-binding protein all have been localized to the α-subunit of GP Ib (reviewed in ref. 9). With the exception of a potential signaling pathway through the GP Ibβ subunit (29), functions for the other subunits of the complex have been associated only with increased efficiency of complex assembly and translocation to the plasma membrane surface (30, 31). Moreover, the *in vivo* role of the GP V subunit can be debated with two laboratories independently reporting GP V null mice. One group concludes a murine knockout of GP V has no apparent phenotypic consequence (32), whereas a second group suggests GP V may be a negative modulator of platelet activation as their work suggests platelets devoid of GP V are hyper-responsive to thrombin (33). In either case, the functional contribution of the GP Ibα subunit to normal platelet biology is clearly established and further substantiated by our results characterizing GP Ibα^{null} mice.

The murine Bernard-Soulier syndrome was rescued by expression of a human GP Ibα transgene. GP Ibα^{null} mice expressing the human transgene have a normal bleeding time, which presumably illustrates the ability of human GP Ibα to bind mouse von Willebrand factor. The correction of the abnormal platelet morphology with the expression of a human transgene illustrates the role of GP Ibα in platelet morphogenesis and, more specifically, that residues of GP Ibα responsible for normal platelet formation and morphology are conserved between mouse and human receptors. The expression of the human transgene did increase the platelet count as compared with GP Ibα^{null} mice, but did not restore the platelet count to levels observed in the wild-type controls presented in Table 1. Several explanations could explain a partial correction of the platelet count. First, circulating platelet counts vary among mouse strains ranging from 1.1×10^6 to 1.6×10^6 per μl of whole blood (34, 35). The GP Ibα^{null} mice are a combination of the original ES cell strain, 129/SvJ, crossed with Swiss Black. The original human transgene was generated in B6×SJL mice but was later crossed with BALB/c mice whose normal count is reported to be $1.1 \times 10^6/\mu$l (34). Thus, strain variation in the absence of generating a new congenic strain invalidates a strict comparison of platelet numbers. However, the mouse strain influence among the three genotypes of GP Ibα mice (Table 1) is probably minimal because these counts were obtained from siblings generated from intracrosses of GP Ibα^{het} mice.

Animal models of platelet dysfunction, such as the mouse model of the Bernard-Soulier syndrome or the recently described Glanzmann thrombasthenia (28), represent valuable resources for platelet experimentation (12). As anucleate fragments of cytoplasm, platelets cannot be experimentally manipulated by using strategies commonly employed for cultured cells in an *in vitro* setting. The release of platelets from the mature megakaryocyte and the platelet response at sites of vascular injury are both highly specialized cellular events performed exclusively by megakaryocytes and platelets. However, the use of a murine model to study platelet biology, or specifically the GP Ib-IX-V complex, is an opportunity to manipulate experimentally the molecular events and processes that are unique to the megakaryocyte and platelet. Thus, the use of such models provides new directions for physiologic and pathologic information of *in vivo* megakaryocyte and platelet function.

We acknowledge the Sam and Rose Stein Charitable Trust for the establishment of the DNA Core Facility within the Department of Molecular and Experimental Medicine at The Scripps Research Institute. This work was supported by Grants HL-50545 and HL-42846 from the Heart, Lung, and Blood Institute of the National Institutes of Health.

1. Bernard, J. & Soulier, J. P. (1948) *Semin. Hosp. Paris* **24,** 3217–3233.
2. Caen, J. P., Nurden, A. T., Jeanneau, C., Michel, H., Tobelem, G., Levy-Toledano, S., Sultan, Y., Valensi, F. & Bernard, J. (1976) *J. Lab. Clin. Med.* **87,** 586–596.
3. Lopez, J. A., Andrews, R. K., Afshar-Kharghan, V. & Berndt, M. C. (1998) *Blood* **91,** 4397–4418.
4. Nurden, A. T., Dupuis, D., Kunicki, T. J. & Caen, J. P. (1981) *J. Clin. Invest.* **67,** 1431–1440.
5. Nurden, A. T., Didry, D. & Rosa, J.-P. (1983) *Blood Cells* **9,** 333–358.
6. Weiss, H. J., Tschopp, T. B., Baumgartner, H. R., Sussman, I. I., Johnson, M. M. & Egan, J. J. (1974) *Am. J. Med.* **57,** 920–925.
7. George, J. N., Nurden, A. T. & Phillips, D. R. (1984) *N. Engl. J. Med.* **311,** 1084–1098.
8. Savage, B., Almus-Jacobs, F. & Ruggeri, Z. M. (1998) *Cell* **94,** 657–666.
9. Ware, J. (1998) *Thromb. Haemostasis* **79,** 466–478.
10. Howard, M. A., Hutton, R. A. & Hardisty, R. M. (1973) *Br. Med. J.* **2,** 586–588.
11. Najean, Y. & Lecompte, T. (1995) *Semin. Thromb. Hemostasis* **21,** 294–304.
12. Jackson, C. W. (1989) *Blood Cells* **15,** 237–253.
13. Young, G., Luban, N. L. & White, J. G. (1999) *Am. J. Hemat.* **61,** 62–65.
14. Ware, J., Russell, S. & Ruggeri, Z. M. (1997) *Blood Cells Mol. Dis.* **23,** 292–301.
15. Fujita, H., Hashimoto, Y., Russell, S., Zieger, B. & Ware, J. (1998) *Blood* **92,** 488–495.
16. Southern, E. M. (1975) *J. Mol. Biol.* **98,** 503–517.
17. Sambrook, J., Fritsch, E. F. & Maniatis, T. (1987) in *Molecular Cloning: Book 1*, ed. Nolan, C. (Cold Spring Harbor Lab. Press, Plainview, NY), pp. 7.1–7.87.
18. Sambrook, J., Fritsch, E. F. & Maniatis, T. (1989) *Molecular Cloning: A Laboratory Manual* (Cold Spring Harbor Lab. Press, Plainview, NY).
19. Ware, J., Russell, S. R., Marchese, P. & Ruggeri, Z. M. (1993) *J. Biol. Chem.* **268,** 8376–8382.
20. Handa, M., Titani, K., Holland, L. Z., Roberts, J. R. & Ruggeri, Z. M. (1986) *J. Biol. Chem.* **261,** 12579–12585.
21. Hourdille, P., Pico, M., Jandrot-Perrus, M., Lacaze, D., Lozano, M. & Nurden, A. T. (1990) *Br. J. Haematol.* **76,** 521–530.
22. Vyas, P., Ault, K., Jackson, C. W., Orkin, S. H. & Shivdasani, R. A. (1999) *Blood* **93,** 2867–2875.
23. Cunningham, J. G., Meyer, S. C. & Fox, J. E. (1996) *J. Biol. Chem.* **271,** 11581–11587.
24. Takahashi, R., Sekine, N. & Nakatake, T. (1999) *Blood* **93,** 1951–1958.
25. Tsakiris, D. A., Scudder, L., Hodivala-Dilke, K., Hynes, R. O. & Coller, B. S. (1999) *Thromb. Haemostasis* **81,** 177–188.
26. Corash, L. (1989) *Blood Cells* **15,** 81–107.
27. Grottum, K. A. & Solum, N. O. (1969) *Br. J. Haematol.* **16,** 277–290.
28. Hodivala-Dilke, K. M., McHugh, K. P., Tsakiris, D. A., Rayburn, H., Crowley, D., Ullman-Cullere, M., Ross, F. P., Coller, B. S., Teitelbaum, S. & Hynes, R. O. (1999) *J. Clin. Invest.* **103,** 229–238.
29. Calverley, D. C., Kavanagh, T. J. & Roth, G. J. (1998) *Blood* **91,** 1295–1303.
30. Lopez, J. A., Leung, B., Reynolds, C. C., Li, C. Q. & Fox, J. E. B. (1992) *J. Biol. Chem.* **267,** 12851–12859.
31. Meyer, S. C. & Fox, J. E. (1995) *J. Biol. Chem.* **270,** 14693–14699.
32. Kahn, M. L., Diacovo, T. G., Bainton, D. F., Lanza, F. & Coughlin, S. R. (1999) *Blood* **94,** 4112–4121.
33. Ramakrishnan, V., Reeves, P. S., DeGuzman, F., Deshpande, U., Ministri-Madrid, K., Dubridge, R. B. & Phillips, D. R. (1999) *Proc. Natl. Acad. Sci. USA* **96,** 13336–13341.
34. Jackson, C. W., Steward, S. A., Chenaille, P. J., Ashmun, R. A. & McDonald, T. P. (1990) *Blood* **76,** 690–696.
35. Levin, J. & Ebbe, S. (1994) *Blood* **83,** 3829–3831.